

# Double-slit experiment in momentum space

I. P. Ivanov,<sup>1,\*</sup> D. Seipt,<sup>2,3,†</sup> A. Surzhykov,<sup>4,5,‡</sup> and S. Fritzsche<sup>2,3,§</sup>

<sup>1</sup>*CFTP, Instituto Superior Técnico, Universidade de Lisboa, av. Rovisco Pais 1, 1049-001, Lisboa, Portugal*

<sup>2</sup>*Helmholtz Institut Jena, D-07743 Jena, Germany*

<sup>3</sup>*Theoretisch-Physikalisches Institut, Friedrich-Schiller-Universität Jena, D-07743 Jena, Germany*

<sup>4</sup>*Physikalisch-Technische Bundesanstalt, D-38116 Braunschweig, Germany*

<sup>5</sup>*Technische Universität Braunschweig, D-38106 Braunschweig, Germany*

Young's classic double-slit experiment demonstrates the reality of interference when waves and particles travel simultaneously along two different spatial paths. Here, we propose a double-slit experiment in momentum space. We show that elastic scattering of vortex electrons proceeds via two paths in momentum space, which are well localized and well separated from each other. For such vortex beams, the (plane-wave) amplitudes along the two paths acquire adjustable phase shifts and produce interference fringes in the final angular distribution. We argue that this experiment can be realized with the present day technology. We show that it gives experimental access to the Coulomb phase, a quantity which plays an important role in all charged particle scattering but which usual scattering experiments are insensitive to.

*Introduction.* Young's seminal double-slit experiment demonstrates the interference of – classical or quantum – amplitudes if the wave propagate along (two) different spatial paths [1]. A wave emitted from some local source passes through two narrow slits in a plate, located at coordinates  $r_a$  and  $r_b$ , and interferes with itself on a distant screen, cf. upper panel of Fig. 1. If the transition amplitudes from the source to a given point on the screen along the two paths are  $f_a$  and  $f_b$ , the intensity profile on the screen is  $|f_a + f_b|^2 = |f_a|^2 + |f_b|^2 + 2\text{Re}(f_a f_b^*)$ , and the interference term produces a spatially periodic signal on the screen. Such interference fringes have been observed not only for photons but also for electrons, atoms [2], and even large organic molecules [3]. Moreover, any modification of the physical conditions along either path probed by these particles gives rise to a shift in the interference pattern, which is the basis of numerous interferometric techniques [1].

A similar situation occurs frequently in collision experiments when an initial state evolves into a final state via different intermediate states, such as different excited states of an atom or different virtual particles in high-energy collisions. For example, elastic scattering of charged hadrons may proceed via purely electromagnetic or purely strong interactions, which interfere in the cross section. In such cases, one observes interference between amplitudes with the same initial and final state kinematics but with different state-space evolution.

In this Letter, we propose a purely momentum-space analog of the Young's double-slit set-up, which exhibits interference between two amplitudes with identical space-state evolution but with different combinations of momenta. Such an experiment must involve a scattering process which brings an initial state to the final state along two distinct, well-separated paths in the momentum space, as illustrated in the lower panel of Fig. 1. Each path resembles a plane-wave scattering with its own momentum transfer, but the final-state kinematics for all

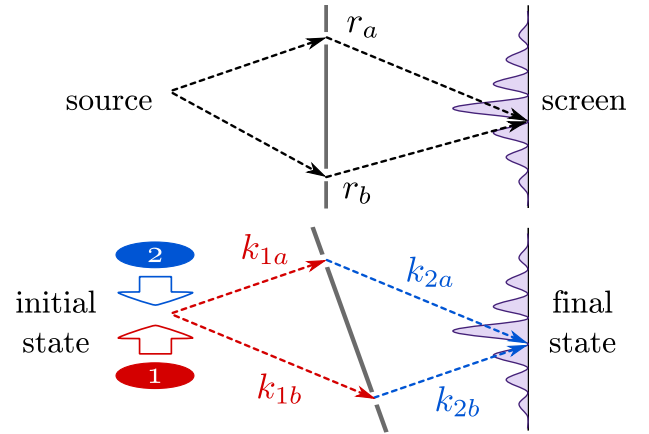


FIG. 1: Schematic illustration of the Young's experiment in the coordinate space (upper pane) and of the proposed double-slit experiment in momentum space (lower pane). In the latter case, we stress that, in the collision of specially prepared wave-packets, only two momentum combinations lead to a given final state.

particles involved must be identical in order for interference to take place. We will show that this peculiar set-up is naturally realized in elastic scattering of Bessel vortex electron beams [5] which were suggested in [6] and recently realized experimentally [7]. As an application of this momentum-space interferometry, we propose to directly access the Coulomb phase, a quantity that affects all charged-particle scattering processes and has been a subject of debates but which has never been measured experimentally.

*The idea.* Consider elastic scattering of two electrons, each represented by a monochromatic wave-packet

$$\psi_i(\vec{r}) = \int d^3k_i a_i(\vec{k}_i) \exp(i\vec{k}_i \vec{r}), \quad (1)$$

with the Fourier amplitude  $a_i(\vec{k}_i)$  being a compact function centered at an average momentum  $\langle \vec{k}_i \rangle$ . Scattering

of two such electrons into a final plane-wave state with momenta  $k'_1$  and  $k'_2$  is well approximated by the plane-wave scattering amplitude  $\mathcal{M}(\langle k_1 \rangle, \langle k_2 \rangle; k'_1, k'_2)$ , the cross sections being proportional to its square,  $d\sigma \propto |\mathcal{M}|^2$ . In momentum space, this process is analogous to a *single-slit* experiment.

To propose a double-slit experiment in momentum space, we select an axis  $z$  and assume that each initial electron is a monochromatic superposition of plane waves with equal longitudinal momentum  $p_z$ , equal modulus of the transverse momentum  $\varkappa$ , but with different azimuthal angles:

$$a_i(\vec{k}_i) \propto \delta(k_{iz} - p_z) \delta(|\mathbf{k}_i| - \varkappa_i) e^{i\ell_i \phi_i}, \quad i = 1, 2. \quad (2)$$

Here and below, transverse vectors are denoted with bold letters. Such states are known as Bessel vortex states, or twisted electrons, [5]. The parameter  $\ell$  can be adjusted experimentally and plays the role of approximately conserved orbital angular momentum with respect to the average propagation direction. Twisted electrons with energies up to 300 keV are now routinely created and manipulated, and are used as novel probes in microscopy [8].

If the two twisted electrons are brought in collision, they can scatter elastically into a final state with momenta  $k'_1$  and  $k'_2$ . Because of momentum conservation, only two plane-wave components with initial momenta  $k_{1a}, k_{2a}$  and  $k_{1b}, k_{2b}$  lead to this final state. The total scattering amplitude is then written as a coherent sum of two plane-wave amplitudes:

$$f \propto c_a \mathcal{M}_a + c_b \mathcal{M}_b, \quad \mathcal{M}_{a,b} = \mathcal{M}(k_{1a,b}, k_{2a,b}; k'_1, k'_2). \quad (3)$$

These two kinematical configurations correspond to different momentum transfers  $q = k_1 - k'_1$ :  $q_a \neq q_b$ . The coefficients  $c_a$  and  $c_b$  in (3) depend both on the initial wave packets and on the final momenta. In particular, by scanning over the allowed region of  $k'_1$  and  $k'_2$ , one can change the relative phase between  $c_a$  and  $c_b$  and observe a periodically varying intensity pattern in the momentum space. The exact position of this pattern in the final-state momentum space is sensitive to the phase difference between  $\mathcal{M}_a$  and  $\mathcal{M}_b$ . This is analogous to the intensity stripes seen on a distant screen in the usual double-slit experiment.

*Elastic scattering of Bessel vortex electrons.* We describe the elastic scattering of two Bessel vortex electrons within the fully relativistic quantum-electrodynamical framework. Details of this calculations will be reported in [9]; here, we briefly outline the procedure. Each initial electron is taken as the exact monochromatic solution of the Dirac equation with definite energy  $E_i$ , longitudinal momentum  $k_{iz}$ , helicity  $\lambda_i$ , and the half-integer total angular momentum  $m_i$ . In this work, we use the expressions from [10]; alternative forms of these solutions also exist [11, 12]. We assume that the two colliding vortex

electrons are aligned, that is, they are defined with respect to the same  $z$  axis. We then select the reference frame in which the longitudinal momenta are balanced:  $k_{2z} = -k_{1z}$ , but where the other parameters can still be different from each other:  $m_1 \neq m_2$ ,  $\varkappa_1 \neq \varkappa_2$ , and therefore  $E_1 \neq E_2$ .

The two final electrons are plane waves with four-momenta  $k'_1$  and  $k'_2$ . Their longitudinal momenta are also balanced,  $k'_{2z} = -k'_{1z}$ , and their energies satisfy  $E'_1 + E'_2 = E_1 + E_2$ . The final transverse momenta, however, are *not* required to sum up to zero or to any fixed vector, because the initial electrons do not carry definite transverse momenta. The only kinematical restriction is that the total final transverse momentum  $\mathbf{K}$  lies within a ring that is defined by  $\varkappa_1$  and  $\varkappa_2$  [13]:

$$|\varkappa_1 - \varkappa_2| \leq |\mathbf{K}| \leq \varkappa_1 + \varkappa_2, \quad \mathbf{K} = \mathbf{k}'_1 + \mathbf{k}'_2. \quad (4)$$

For such a scattering of two Bessel beams, the final phase space grows from the single-particle angular distribution  $d\Omega$  or the transverse momentum  $d^2\mathbf{k}'_1$  to the four-dimensional transverse momentum space  $d^2\mathbf{k}'_1 d^2\mathbf{k}'_2 = d^2\mathbf{k}'_1 d^2\mathbf{K}$ . As a consequence, further information can be extracted from the structures in the final kinematical distributions.

Next, we express the twisted electron scattering matrix element  $S_{tw}$  as the integral of the plane-wave matrix element  $S_{PW}$  over the initial electron wave function:

$$S_{tw} \propto \int d^3k_1 d^3k_2 a_{\varkappa_1 m_1}(\vec{k}_1) a_{\varkappa_2 m_2}(\vec{k}_2) S_{PW}. \quad (5)$$

Here

$$S_{PW} \propto \delta^{(4)}(k_1 + k_2 - k'_1 - k'_2) \cdot \mathcal{M}(k_1, k_2; k'_1, k'_2) \quad (6)$$

and the invariant amplitude  $\mathcal{M}$  is calculated according to the standard Feynman rules [14]. For vortex beams, in practice, the calculations of the scattering cross section require special care since the regularization and normalization prescriptions, as well as the definition of the flux differ from the plane-wave case [12, 13, 15, 16]. In our calculations, all these technical aspects are taken into account, but we omit them here for brevity; they will be fully presented in [9]. The integral (5) contains equal number of integrations and delta functions, and it can be worked out exactly. For each  $\mathbf{K}$ , it receives contributions from *exactly two* choices of the initial transverse momenta  $\mathbf{k}_{1,2}$  with moduli  $\varkappa_{1,2}$  and the azimuthal angles  $\phi_{1a} = \phi_K + \delta_1$ ,  $\phi_{2a} = \phi_K - \delta_2$  and  $\phi_{1b} = \phi_K - \delta_1$ ,  $\phi_{2b} = \phi_K + \delta_2$ , where

$$\delta_{1,2} = \arccos \left( \frac{\varkappa_{1,2}^2 + \mathbf{K}^2 - \varkappa_{2,1}^2}{2\varkappa_{1,2}|\mathbf{K}|} \right) \quad (7)$$

are the internal angles of the triangle with sides  $\varkappa_1$ ,  $\varkappa_2$ ,  $|\mathbf{K}|$ . The area of this triangle is denoted by  $\Delta =$

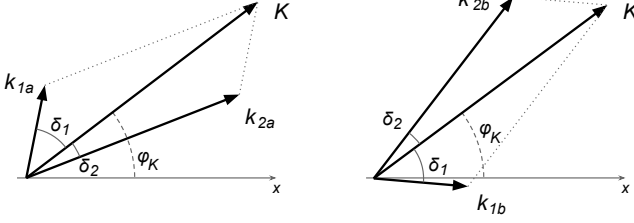


FIG. 2: The two kinematical configurations in the transverse plane that satisfy momentum conservation laws in the two Bessel state scattering.

$|\mathbf{K}|\varkappa_1 \sin \delta_1/2$ . These two configurations are shown in Fig. 2.

Squaring the matrix element, regularizing it, and dividing by the flux, we obtain the following expression for the twisted electron cross section:

$$d\sigma_{tw} \propto |\mathcal{J}|^2 d^2\mathbf{k}'_1 d^2\mathbf{k}'_2 = |\mathcal{J}|^2 d^2\mathbf{k}'_1 d^2\mathbf{K}, \quad (8)$$

where

$$\begin{aligned} \mathcal{J} &= \int d^2\mathbf{k}_1 d^2\mathbf{k}_2 \delta^{(2)}(\mathbf{k}_1 + \mathbf{k}_2 - \mathbf{K}) \\ &\times \delta(|\mathbf{k}_1| - \varkappa_1) \delta(|\mathbf{k}_2| - \varkappa_2) \\ &\times e^{im_1\phi_1 - im_2\phi_2} \mathcal{M}(k_1, k_2; k'_1, k'_2) \\ &= e^{i(m_1 - m_2)\phi_K} \frac{\varkappa_1 \varkappa_2}{2\Delta} \times \\ &\times \left[ \mathcal{M}_a e^{i(m_1\delta_1 + m_2\delta_2)} + \mathcal{M}_b e^{-i(m_1\delta_1 + m_2\delta_2)} \right]. \end{aligned} \quad (9)$$

Here,  $\mathcal{M}_a$  and  $\mathcal{M}_b$  are the two plane-wave scattering amplitudes as in Eq. (3), which are calculated for the two distinct initial momentum configurations shown in Fig. 2. They correspond to the same relativistic  $s$ -invariant but two distinct  $t$ -invariants  $t_{a,b} = (k_{1a,b} - k'_1)^2 = (k_{2a,b} - k'_2)^2$ , whose difference is

$$t_a - t_b = 2\mathbf{k}'_1(\mathbf{k}_{1a} - \mathbf{k}_{1b}) = 4|\mathbf{k}'_1|\varkappa_1 \sin \delta_1 \sin(\phi'_1 - \phi_K). \quad (11)$$

*Interference fringes.* To get qualitative understanding, consider (8) in the ultrarelativistic small scattering angle approximation:  $|\mathbf{k}_i|, |\mathbf{k}'_i| \ll k_z$ . Unlike the plane-wave scattering, where the total transverse momentum fulfills the condition  $\mathbf{K} = \mathbf{k}'_1 + \mathbf{k}'_2 = 0$ , we have here an extra dimension to look at: the  $\mathbf{K}$ -distribution at fixed  $\mathbf{k}'_1$ . This distribution fills the ring defined by (4) and display interference fringes. For high electron energies and small scattering angles, the helicity amplitude can be approximated by

$$\mathcal{M} = 8\pi\alpha_{em} \frac{s}{t} e^{-i\lambda_1(\phi_1 - \phi'_1)} e^{i\lambda_2(\phi_2 - \phi'_2)} \delta_{\lambda_1\lambda'_1} \delta_{\lambda_2\lambda'_2}. \quad (12)$$

Substituting it into (10), we obtain, for the unpolarized

case,

$$\begin{aligned} \frac{1}{4} \sum_{\lambda_i} |\mathcal{J}|^2 &= 64\pi^2 \alpha_{em}^2 s^2 \frac{\varkappa_1^2 \varkappa_2^2}{4\Delta^2} \\ &\times \left[ \frac{1}{t_a^2} + \frac{1}{t_b^2} + \frac{2}{t_a t_b} \cos(2m_1\delta_1 + 2m_2\delta_2) \cos \delta_1 \cos \delta_2 \right]. \end{aligned} \quad (13)$$

By detecting electrons with different  $\mathbf{k}'_2$  at fixed  $|\mathbf{k}'_1|$ , we can scan the ring (4). As seen from (7), the angles  $\delta_i$  change, and the last term in (13) oscillates, producing concentric ring structure. These are the characteristic interference fringes of Young's double-slit experiment but now in the *momentum space*.

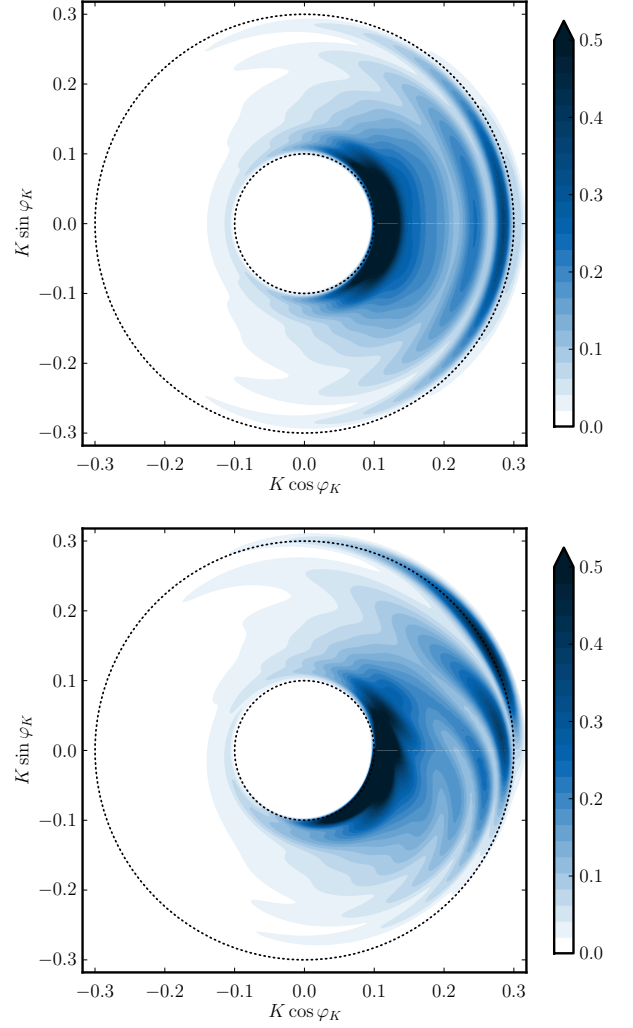


FIG. 3: Differential cross section, in arbitrary units, as a function of  $\mathbf{K}$  for fixed  $\mathbf{k}'_1$  for a choice of parameters (see text). The upper plot is calculated from the purely real Born-level amplitude, while the lower plot takes into account the Coulomb phase (14), with  $\alpha_{em}$  artificially set to 10 to enhance the visibility of the up-down asymmetry.

Before verifying the above analysis with numerical results, we mention that pure Bessel beams are not nor-

malizable and, formally, lead to divergent expressions. However, realistic vortex beams produced in experiment are free from these difficulties. To model them, we follow [16, 17] and replace the singular Fourier components  $a(\vec{k})$  as in (2) with their Gaussian-distributed Fourier components  $\tilde{a}(\vec{k}) = \int d\mathbf{x} f(\mathbf{x}) a_{\mathbf{x}}(\vec{k})$ , where  $f(\mathbf{x}) \propto \exp[-(\mathbf{x} - \bar{\mathbf{x}})^2/2\sigma^2]$ . This leads to the corresponding averaging over a region of  $k_{1z}$  and  $k_{2z}$ , so that we get a narrow distribution over final  $K_z$  peaked at  $K_z = 0$ , over which we further integrate the cross section.

The upper pane of Fig. 3 shows the numerically obtained cross sections with the following parameters:  $E_1 = 2.1$  MeV,  $\bar{x}_1 = 200$  keV,  $\bar{x}_2 = 100$  keV,  $\sigma_i = \bar{x}_i/20$ ,  $|\mathbf{k}'_1| = 500$  keV,  $m_1 = 1/2$ ,  $m_2 = 13/2$ . In this plot,  $\mathbf{k}'_1$  is directed to the right. One sees the interference fringes as well as the strong left-right asymmetry, originating from the  $t$ -dependence of (13). The plot is symmetric with regard to the horizontal line because the cross section contains no term proportional to  $\sin(\phi'_1 - \phi_K)$ .

*Accessing the Coulomb phase.* The two-slit interferometry in momentum space as proposed here provides direct access to a quantity which cannot be measured in the usual plane-wave scattering: the phase of the (complex) scattering amplitude, or more accurately, its dependence on the momentum transfer squared  $t$ . For elastic scattering of charged particles, this phase is known as the Coulomb phase. If we write the amplitude as  $\mathcal{M} = |\mathcal{M}|e^{i\zeta}$ , one obtains for ultrarelativistic same-sign charged particles

$$\zeta = \zeta_0 + \alpha_{em} \ln(1/|t|), \quad (14)$$

where  $\zeta_0$  is the unobservable overall phase which depends on the infrared regularization.

The Coulomb phase cannot be measured experimentally because it drops out of the plane-wave cross section. But it plays an important role in elastic scattering of charged hadrons. Its amplitude receives contributions from the strong and electromagnetic interactions,  $\mathcal{M} = \mathcal{M}_s + \mathcal{M}_{em}$ , which become interrelated at higher orders of the perturbation series. Knowing the Coulomb phase as accurately as possible is needed to probe the large unknown strong phase via the interference between the strong and electromagnetic amplitudes. But the electromagnetic amplitude itself involves intermediate excited hadronic states, which further complicates its calculation. This issue sparked debates back in 1960's [18–23], and is still discussed today, in the context of elastic  $pp/p\bar{p}$  and deep-inelastic scattering [24–28].

The two-slit interferometry in momentum space may lead to the first ever measurement of the  $t$ -dependence of the Coulomb phase. This occurs since the interference term in (3) is sensitive to the phase difference,

$$d\sigma_{int} \propto 2|\mathcal{M}_a||\mathcal{M}_b|\text{Re}\left[c_a c_b^* e^{i(\zeta_a - \zeta_b)}\right], \quad (15)$$

where  $\zeta_a - \zeta_b \approx \alpha_{em} \ln(t_b/t_a)$ . The extra phase difference between  $\mathcal{M}_a$  and  $\mathcal{M}_b$  distorts the interference pattern. The cross section acquires a new term proportional to  $t_a - t_b \propto \sin(\phi'_1 - \phi_K)$  and leads to the up-down asymmetric  $\mathbf{K}$ -distribution, which is entirely due to the  $t$ -dependent Coulomb phase. The lower pane of Fig. 3 shows this asymmetry for the same parameter set as before. Note that here, for the sake of illustration, the effect is greatly exaggerated by setting  $\alpha_{em} = 10$ . For physical  $\alpha_{em}$ , the effect is proportionally smaller, but it can be extracted from the experimentally measured cross section via asymmetry  $A_{\perp} = \int d\sigma_{tw} \sin(\phi'_1 - \phi_K) / \int d\sigma_{tw}$ . Our numerical calculations give  $A_{\perp} = \mathcal{O}(10^{-4} \div 10^{-3})$ , whose smallness is mostly driven by the small  $\alpha_{em}$ . The exact value of  $A_{\perp}$  strongly depends on the details of the initial state; by adjusting them, one can further optimize the sensitivity of this measurement to the Coulomb phase.

*Which-way experiment in the momentum space.* The “which way experiment” is a variation of the classical double-slit experiment, in which a device is placed next to one slit in order to detect whether the particle actually passes through it. Using such a device lets interference disappear or, for non-ideal detection, degrade, displaying the laboratory proof of the reality of quantum-mechanical complementarity [4]. The proposed two-slit experiment in momentum space can also be modified in order to establish a corresponding which-way experiment. The idea is to consider *inelastic* scattering,  $ee \rightarrow ee\gamma$ , in which a sufficiently energetic bremsstrahlung photon is detected in coincidence with the scattered electrons. Since the two interfering plane-wave configurations have different initial momenta, say  $k_{1a}$  and  $k_{1b}$ , detection of the bremsstrahlung photon close to the direction of  $k_{1a}$  gives preference to this “slit” in the momentum space. Selecting different photons, one can change the efficiency of the “which-way detection”, and the interference fringe contrast must vary accordingly.

*Discussion.* The proposed experiment can be realized with present day beams and detectors. Vortex electrons with energies up to 300 keV and focused to angstrom-size focal spots are now routinely produced and manipulated in electron microscopes [8]. Scattering of two vortex electron beams has not yet been studied experimentally, but it can be readily done once the instrumentation is modified for this purpose. High contrast images of the vortex beams in the focal plane in these experiments suggest that stable alignment of the two beams within the common focal spot can be achieved. With the angstrom-scale focal spot and the kinematical parameters used here, we estimate the scattering probability for each  $ee$  crossing of about  $P \sim \sigma_{tw}/S_{\text{focal}} \sim 10^{-6}$ . With the beam currents of 1 nA, one can set up billions of  $ee$  collision attempts per second resulting in hundreds of detectable scattering events per second. A few hours of observation time will produce a million-event statistics.

In order to construct plots such as Fig. 3, the detectors

must detect scattered electron pairs in coincidence and with sufficient angular resolution, while the electron energy need not to be measured explicitly. From these coincidence measurements, one then slices the full sample of detected  $\mathbf{k}'_1$  and  $\mathbf{k}'_2$  pairs into subsamples with given  $|\mathbf{k}'_1|$ , reconstructs  $\mathbf{K}$ , and plots the events in the  $\mathbf{K}$ -space with respect to the orientation of  $\mathbf{k}'_1$ . A million-event statistics should be enough to detect the interference fringes inside the annular  $\mathbf{K}$ -region. In order to detect a non-zero asymmetry  $A_\perp$  and probe the Coulomb phase, these structures need to be measured with even higher accuracy, which seems challenging at present.

*To conclude*, we proposed the momentum-space analogue of the classical Young's double-slit experiment. When two Bessel vortex electrons scatter elastically, the process is dominated by two plane-wave scattering configurations with different momentum transfers. Just like two slits in the usual Young's interference experiment, these two configurations corresponds to two paths which are well localized and well separated in the momentum space. The two paths acquire adjustable phase difference, their amplitudes sum up coherently and lead to interference fringes in the final state angular distribution. We showed, in particular, that this interference allows for the first ever experimental investigation of the Coulomb phase. We also proposed the which-way modification of this experiment, with a bremsstrahlung photon playing the role of a detecting device with imperfect efficiency. We argued that the proposed momentum-space double-slit experiment can be realized with the present day technology.

The work of I.P.I. was supported by the Portuguese *Fundação para a Ciência e a Tecnologia* (FCT) through the FCT Investigator contract IF/00989/2014/CP1214/CT0004 under the IF2014 Programme, as well as under contracts UID/FIS/00777/2013 and CERN/FIS-NUC/0010/2015, which are partially funded through POCTI, COMPETE, QREN, and the EU. I.P.I. is also thankful to Helmholtz Institut Jena for hospitality during his stay as a Visiting Professor funded by the ExtreMe Matter Institute EMMI, GSI Helmholtzzentrum für Schwerionenforschung, Darmstadt.

---

\* E-mail: igor.ivanov@tecnico.ulisboa.pt

- <sup>†</sup> E-mail: d.seipt@gsi.de
- <sup>‡</sup> E-mail: andrey.surzhykov@ptb.de
- <sup>§</sup> E-mail: s.fritzsche@gsi.de
- [1] M. Born, E. Wolf, "Principles of optics", Cambridge University Press, 7th edition (1999).
- [2] O. Carnal and J. Mlynek, Phys. Rev. Lett. **66**, 2689 (1991).
- [3] S. Gerlich, S. Eibenberger, M. Tomandl, S. Nimmrichter, K. Hornberger, P. J. Fagan, J. Tüxen, M. Mayor, and M. Arndt, Nature Comm. **2**, 263 (2011).
- [4] P. Mittelstaedt, A. Prieur, R. Schieder, Foundations of Physics **17**, 891 (1987).
- [5] J. Harris et al, Nature Physics **11**, 629 (2015).
- [6] K. Y. Bliokh, Y. P. Bliokh, S. Savel'ev, and F. Nori, Phys. Rev. Lett. **99**, 190404 (2007).
- [7] M. Uchida and A. Tonomura, Nature **464**, 737 (2010); J. Verbeeck, H. Tian, and P. Schlattschneider, Nature **467**, 301 (2010). B. J. McMorran *et al.*, Science **331**, 192 (2011).
- [8] G. Guzzinati, "Exploring electron beam shaping in transmission electron microscopy", PhD Thesis, University of Antwerp (2015).
- [9] I. P. Ivanov, S. Fritzsche, D. Seipt, and A. Surzhykov, *in preparation*.
- [10] V. G. Serbo, I. P. Ivanov, S. Fritzsche, D. Seipt, and A. Surzhykov, Phys. Rev. A **92**, 012705 (2015).
- [11] K. Y. Bliokh, M. R. Dennis, and F. Nori, Phys. Rev. Lett. **107**, 174802 (2011).
- [12] D. V. Karlovets, Phys. Rev. A **86**, 062102 (2012).
- [13] I. P. Ivanov, Phys. Rev. D **83**, 093001 (2011).
- [14] V. B. Berestetsky, E. M. Lifshitz, and L. P. Pitaevsky, *Quantum Electrodynamics*, Vol. 4 (Butterworth-Heinemann, 1982).
- [15] U. D. Jentschura and V. G. Serbo, Eur. Phys. J. C **71**, 1571 (2011).
- [16] I. P. Ivanov, Phys. Rev. D **85**, 076001 (2012).
- [17] I. P. Ivanov and V. G. Serbo, Phys. Rev. A **84**, 033804 (2011).
- [18] H. A. Bethe, Annals Phys. **3**, 190 (1958).
- [19] W. B. Rolnick, Phys. Rev. **148**, 1539 (1966).
- [20] J. Rix and R. M. Thaler, Phys. Rev. **152**, 1357 (1966).
- [21] M. M. Islam, Phys. Rev. **162**, 1426 (1967).
- [22] L. D. Solov'ev, Sov. Phys. JETP **22**, 205 (1966).
- [23] Geoffrey B. West and D. R. Yennie Phys. Rev. **172**, 1413 (1968).
- [24] R. Cahn, Z. Phys. C **15**, 253 (1982).
- [25] O. V. Selyugin, Phys. Rev. D **60**, 074028 (1999).
- [26] B. Z. Kopeliovich and A. V. Tarasov, Phys. Lett. B **497**, 44 (2001).
- [27] V. A. Petrov, E. Predazzi and A. Prokudin, Eur. Phys. J. C **28**, 525 (2003).
- [28] I. M. Dremin, Phys. Usp. **56**, 3 (2013) [Usp. Fiz. Nauk **183**, 3 (2013)]